Geomechanics and Engineering, *Vol. 38, No. 2 (2024) 191-203*
https://doi.org/10.12989/gae.2024.38.2.191

Assessment of creep improvement of organic soil improved by stone columns

Kumail R. Al-Khafaji[a], Mohammed Y. Fattah* and Makki K. Al-Recaby[b]

Department of Civil Engineering, University of Technology, Baghdad, Iraq

(*Received May 16, 2022, Revised May 14, 2024, Accepted July 15, 2024*)

Abstract. One of the issues with clayey soils, particularly those with significant quantities of organic matter, is the creep settling problem. Clay soils can be strengthened using a variety of techniques, one of which is the use of stone columns. Prior research involved foundation loading when the soil beds were ready and confined in one-dimensional consolidation chambers. In this study, a particular methodology is used to get around the model's frictional resistance issue. Initially, specimens were prepared via static compaction, and they were then re-consolidated inside a sizable triaxial cell while under isotropic pressure. With this configuration, the confining pressure can be adjusted, the pore water pressure beneath the foundation can be measured, and the spacemen's lateral border may be freely moved. This paper's important conclusions include the observation that secondary settlement declines with area replacement ratio. Because of the composite ground's increasing stiffness, the length to diameter ratio (l/d) and the stone column to sample height ratio (Hc/Hs) both increase. The degree of improvement varies from 12.4 to 55% according to area replacement ratio and (l/d) ratio.

Keywords: creep improvement factor; ground improvement; organic soil; secondary settlement; stone column

1. Introduction

Due to its ability to strengthen unstable and deficient soils, stone columns have a wide range of significant applications. Soft clays, silts, organic soils, and loose granular beds can all be effectively improved with it. Granular piles increase the load-bearing capacity of soft ground while also lowering settling to a manageable level. Additionally, they speed up the primary consolidation rate, which means that a significant portion of the post-construction settlement may come from secondary settlement (creep). In addition, some soft organic soils provide a premium on secondary settlement (e.g., Hameedi *et al.* 2020; Basha *et al.* 2024).

It is evident from the research conducted on laboratory studies, analytical models, numerical simulations, field studies, efficiency improvements, and quality control (Hughes and Withers 1974, Aboshi *et al.* 1979, Balaam and Booker 1981, Barksdale and Bachus 1983, McKelvey 2002, McKelvey *et al.* 2004, McCabe *et al.* 2009, Fattah *et al.* 2011, 2016, 2017, Mohamed *et al.* 2023). Under raft foundations with low to medium weights, stone columns are typically utilized. It has, nevertheless, lately been utilized beneath tiny insulated foundations and strip foundations. The bearing capacity and primary settlement features were the main focus of numerous earlier investigations , e.g., (Ambily and Gandhi 2007, Barksdale and Bachus 1983, Mitchell and Huber 1985, Watts *et al.* 2000, Fattah *et al.* 2015), on the contrary, little researches were done on the issue of secondary settlement.

The homogeneity of load and geometry is the foundation of the unit cell idea. Similar to one-dimensional compression, a rigid platform loads the unit cell vertically, causing it to be laterally constrained and the horizontal surface to be uniformly stretched vertically. This has led to the development of multiple methods for assessing composite ground settlement (Priebe 1976, 1995, Aboshi *et al.* 1979, Van Impe 1983, Shahu *et al.* 2000, Kumar and Samanta 2020, etc.).

Because it produces better findings than in situ observations for infinite groups, this approach is more commonly utilized. However, because group interaction effects are complicated, the accuracy decreases when tiny group configurations are used (McCabe *et al.* 2009).

Settlement design methods are related to the direct estimation of a creep improvement factor, $n_{creep}= \delta_{untreated}/\delta_{treated}$ defined as the ratio of the settlement of untreated (no column) ground settlement divided by the settlement of ground treated ground. This creep improvement factor can, in turn, be used to estimate the settlement of improved soil.

The properties of the original soil have a significant impact on performance and efficiency in addition to granular column characteristics, such as the ratio of column length to diameter (l/d), spacing between columns (s), area replacement ratio (As), stiffness ratio of the column to the surrounding soil (Ec/Es), stress ratio of the column and soil (vc/vs), and the number of supporting columns. The most

*Corresponding author, Professor
E-mail: 40011@uotechnology.edu.iq
[a]Graduate student
E-mail: bce.19.48@grad.uotechnology.edu.iq
[b]Assistant Professor
E-mail: 40139@uotechnology.edu.iq

ISSN: 2005-307X (Print), 2092-6219 (Online)

common reason for short columns (l/d<6) to fail is end bearing failure, while long columns (l/d > 6) typically fail because of bulging (Hughes and Withers 1974).

A novel, simplified approach for calculating the settling of a thick soil layer with creep was developed by Feng and Yin (2020). It is a new, streamlined method that obtains the whole settlement, including consolidation and creep settlement, without the need for laborious numerical procedures. It is suggested to use α = Uzα = Uz as a variable rather than a constant as in earlier research. The new simplified method is based on a mathematical solution for the consolidation analysis of a soil layer to take nonlinear compressibility into consideration. The new simplified method is verified by comparing our calculated values with the finite-element (FE) simulated results in a number of instances involving varying soil strata thicknesses, OCR values, surcharge loadings, and creep parameter values.

In order to quantify the pore water pressure, vertical stress, lateral stress, and coefficient of lateral earth pressure in soil over time, Hameedi *et al*. (2021) devised a multistage oedometer relaxation test. A novel relaxation factor in organic soil is proposed. There are six stages in the test, and each one lasts between ten and thirty minutes, unless the pore water pressure is not lost. Long-term stress relaxation results showed that, after a certain amount of time, there is a linear relationship between the logarithm of time and the growth in stress relaxation.

The behavior of stone columns covered in recycled tires was studied by Lajevardi and Enami (2021), who believe that this material could eventually replace other encasements. In a big box, stone columns with diameters of 66, 80, and 92 mm—one-tenth of the original tire sizes—were tested, and their load-carrying capabilities were examined. According to the findings, the efficacy of the stone column encasement rises with increasing diameter. When single or multiple stone columns are covered in scrap tires, their bearing capacity is increased more than when the columns are made of regular stone. Nonetheless, the geotextile-encased stone column has a higher bearing capability than the other categories. Additional numerical analysis has been done in order to put full-scale reinforced columns into practice. The findings showed that increasing the bearing capacity of stone columns and reducing bulging failure are two benefits of employing recycled tires.

Al-Auqbi *et al*. (2022) discovered a reversible relationship between shear parameters and creep settlement in floating stone columns; however, a direct positive relationship was observed between shear parameters and creep settlement in end-bearing stone columns, with the creep settlement starting at the primary settlement. The creep settlement improvement factor (n) in end-bearing and floating stone columns was influenced by the shear parameters. In floating and end-bearing situations, the n values of the standard creep coefficient were more significant than the n values of the low creep coefficient in forwarded geometric conditions.

Sun *et al.* (2024) developed an analytical model that explained the initial clogging as well as linked time and depth-dependent fouling of stone columns. Degradation analysis and well-aligned case studies demonstrate the precision and dependability of the suggested model. The calculated findings of the present investigation are then compared with the models that are currently in use, and a detailed evaluation of the effects of a number of important parameters on the consolidation behavior is carried out. The findings showed that the consolidation performance is significantly impacted by the initial congestion as well. Additionally, the consolidation process will be noticeably slowed down, especially in the later stages, due to the increase in depth and time-consuming aspects a and b.

Clay soils can be strengthened using a variety of techniques, one of which is the use of stone columns. Prior research involved foundation loading when the soil beds were ready and confined in one-dimensional consolidation chambers. In this study, a particular methodology is used to get around the model's frictional resistance issue. Initially, specimens were prepared via static compaction, and they were then re-consolidated inside a sizable triaxial cell while under isotropic pressure. With this configuration, the confining pressure can be adjusted, the pore water pressure beneath the foundation can be measured, and the spacemen's lateral border may be freely moved. This embodies the originality of the current investigation.

The primary obstacle in the latter scenario is the amount of time needed to measure "pure" long-term creep settlements in soft, low-permeability soils. The present work aims to study the effect of the ratio of length to diameter (l/d), area replacement ratio (As) and the length of the stone column to the height of soil bed (Hc/Hs) on the behavior of floating stone column during the secondary settlement period.

2. Methodology

In the review of previous studies, one-dimensional compaction chambers were used to prepare and restrict soil layers during foundation loading. Two main issues are related to a lack of precise evaluation of settlement performance:

Non-uniformity of soil stiffness properties due to frictional resistance along the boundaries, and

Uncontrolled pore water pressure during foundation loading.

There was a precise process that was followed to prevent these issues. Tests were carried out on disturbed soil that was transported from the sanitary dump site close to the Al-Rustamiya wastewater treatment facility, which is located in Iraq to the southeast of Baghdad. Finding the change in the undrained shear strength over time at various water contents was the first stage. These tests determine how long it takes the remolded soil to strengthen again after the mixing operation and a rest interval. As seen in Fig. 1, it is discovered that the remolded soil needs roughly three days to recover its strength.

The second point was determining the variation of shear strength after 3-day mixing versus different liquidity indices. The results of the variation of the undrained shear strength with different liquidity indices are shown in Fig. 2.

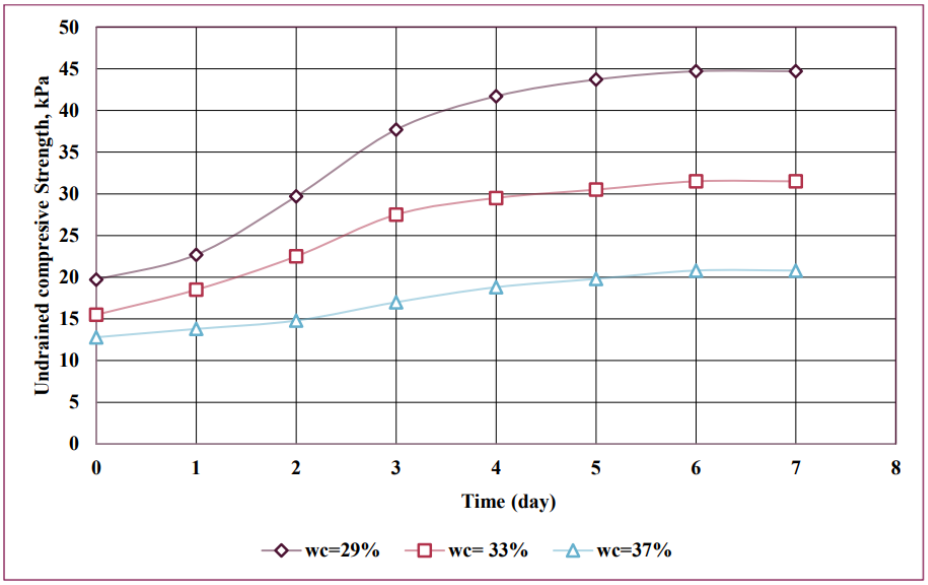

Fig. 1 Variation of the undrained shear strength with time for different moisture contents

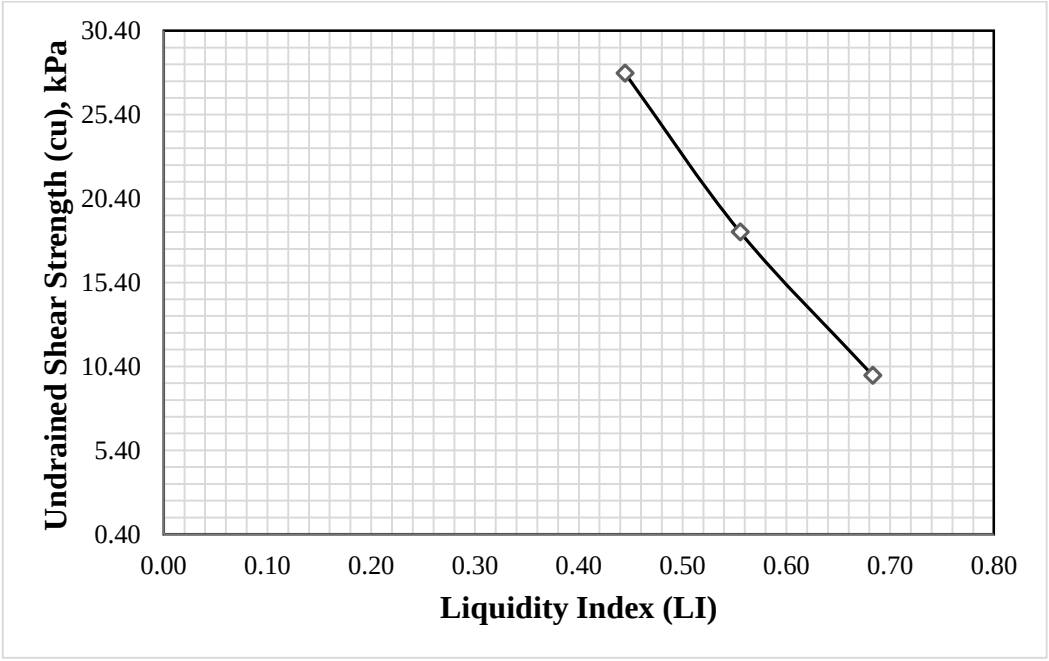

Fig. 2 Variation of the undrained shear strength with liquidity index after 3- day curing

The soil was first prepared by mixing it with 48% moisture content to achieve an undrained compressive strength of 23 kPa (soft state). It was then compacted one-dimensionally in the 100 x 200 mm diameter and height split mold of the triaxial test to achieve a wet density of 1592 kg/m3. Finally, it was re-consolidated inside a sizable triaxial cell under isotropic pressure.

This setup allows controlling the confining pressure, the possibility of measuring the pore water pressure under the foundation, and the freedom of the lateral boundaries of the spacemen. The following parts describe the properties of this triaxial cell spaceman, preparation and procedure associated with it.

2.1 Test equipment

As seen in Fig. 3, a sizable triaxial cell that could test materials with a diameter of 100 mm and a height of 200 mm was employed. To satisfy the particular requirements of the current study, a few unique characteristics were required, which are as follows. For Ko consolidation, separate control over lateral and vertical pressures was offered. Vertical pressure and cell fluid were used to apply confining pressure (σ3). Through the use of an internal loading frame, the force activated by this device placed additional stress on the sample top plate.

Independent foundation loading was applied.

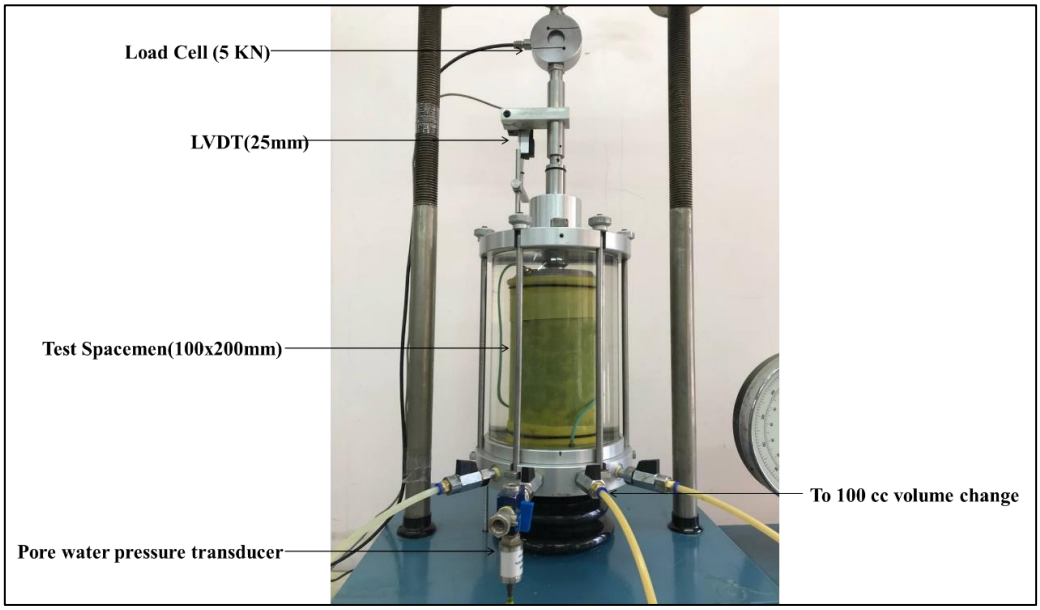

Fig. 3 Triaxial testing machine

Fig. 4 Small model of stone column-soil in the triaxial cell

Foundation loading was achieved using a small, independent 100 mm diameter footing located within the top plate, as illustrated in Fig. 4. The foundation was instrumented with a load cell (640 kPa range) to monitor the contact pressure, located at the center of the footing Fig. 2. The independent foundation and top plate's displacement were measured using a separate 25 mm stroke linear variable differential transformer (LVDT) device. Cell pressure, pore water pressure and the triaxial machine were controlled using manual pressure controllers to apply independent foundation loading. All instrumentation was interfaced with a 16-channel data logger (Wykeham Farrance series 6000) for data acquisition.

A sequence of cell-back pressures that increase with a deference of 10 kPa and step of 100 kPa is used by ASTM D4767-11 to saturate all specimens. All tested samples showed a measured "B" value greater than 0.95, suggesting that the measured "B" value an appropriate degree of saturation

2.2 Column installation

Using a helical drill (10 mm diameter) with a constant speed rate, the borings were carefully drilled and followed by the insertion of a smooth steel tube with the exactly needed diameter. This procedure was necessary to avoid cracking and disturbance of the soil around the hole. A poorly graded basalt aggregate with particles ranging from 1 to 4.75 mm was introduced in stages inside the holes (maintaining a 1:30 scale factor) and compacted employing a free-falling metal rod weighing 1.1 kg through a fixed distance of 90 mm for a series of 10 blows. The rod weight and number of blows were choen by trials. The sale factor was selected based on several previous studies that adopted small scale laboratory test models e.g., Ye *et al*. (2014). Sexton *et al.* (2016) pointed out that while the majority of laboratory-scale testing carried out to date has been informative, it tends to be limited by scale effects and a difficulty in replicating realistic boundary conditions.

Table 1 Material properties

Material	Property	Value	Specification
Organic soil	Particle size, < 75 μm	91%	ASTM D422
	Liquid limit, %	66	ASTM D4318
	Plastic limit, %	30	ASTM D4318
	Plasticity index, %	36	ASTM D4318
	Undrained shear strength Cu, kPa	**23**	ASTM D2166
	Compression index: Cc	0.34	ASTM D2435
	Swelling index: Cs	0.054	ASTM D2435
	Secondary compression index: Cα	0.015	ASTM D2435
	Organic matter (LOI), %	25-30	ASTM D2974
Poorly Graded Basalt Aggregate	Particle size (mm)	1-4.75	ASTM C136
	Friction angle (ϕ), degrees	21o	ASTM D3080

Table 1 Test schedule

Test	Column length, l (mm)	Column diameter, d (mm)	Area replacement ratio, As (%)
T-01	0	0	0
T-02	**80**	2**0**	**4**
T-03	**120**	2**0**	**4**
T-04	**160**	2**0**	**4**
T-05	**80**	**27**	**7.3**
T-06	**120**	**27**	**7.3**
T-07	**160**	**27**	**7.3**
T-08	**80**	38	**14.4**
T-09	**120**	38	**14.4**
T-10	**160**	38	**14.4**

Additionally, Castro *et al*. (2013) have noted that the reconstituted soils used in laboratory testing are not fully representative of natural clay behaviour. There are also difficulties associated with extrapolating long-term performance in the field from short-term laboratory tests (Mitchell and Kelly 2013).

The average dry density of the aggregate was calculated as 1700 kg/m3, assuming a constant hole volume during installation. Cavity was expanded during the compaction process. The same aggregate was compacted into a known volume rigid steel tube; the average dry density was 1590 kg/m3, implying a 7% cavity expansion due to the installation process. Therefore, this calculation was roughly used as a means of ensuring the control of quality between tests. Each column was saturated with de-aired water, and a thin layer of washed fine sand was placed on the top of the column. This layer was used to ensure the uniformity of load acting on the pane of soil as soon as the top of the column. Further soil and basalt aggregate material features are reported in Table 1.

2.3 Testing program

In the testing program, the focus was on the influence of area replacement ratio As and length to diameter ratio l/d, as illustrated in Table 2. Beneath a 100 mm diameter foundation, the column diameters of 20, 27 and 38 mm respectively were used corresponding area replacement ratio of 4, 7.7 and 14.4%, respectively.

The amount of stone replacement is quantified by the area replacement ratio, or Ac/A (Eq. (1)). Granular column cross-sectional area (Ac) can be written as (πdc 2 /4), where dc is the column diameter and (A) is the cross-sectional area (subject to variation in column spacing, s, and column arrangement) of the unit cell with which it is related, as indicated by (C).

$$\frac{\boldsymbol{Ac}}{\boldsymbol{Aa}} = \mathrm{C}\ \left(\frac{Dc}{s}\right)^2 \tag{1}$$

Considering lengths of 80 mm, 120 mm and 160 mm, representing Hc/Hs ratios of 0.4, 0.6 and 0.8, respectively (where Hc and Hs are the lengths of the column and height of specimen, respectively).

The specimen was initially saturated, and the air voids trapped in the soil and column are dissolved by applying confining and back pressure with deference of 10 kPa and step of 100 kPa until the pore water pressure parameter B value of 0.96 is reached, then consolidated isotropically under a confining pressure of 220 kPa and a back-pressure of 100 kPa, which took approximately two days. In contrast, the consolidation was accelerated to 19 hours when a 160 mm column was present.

Isotropic confinement was followed by consolidation on the Ko line, where the effective vertical stress was increased

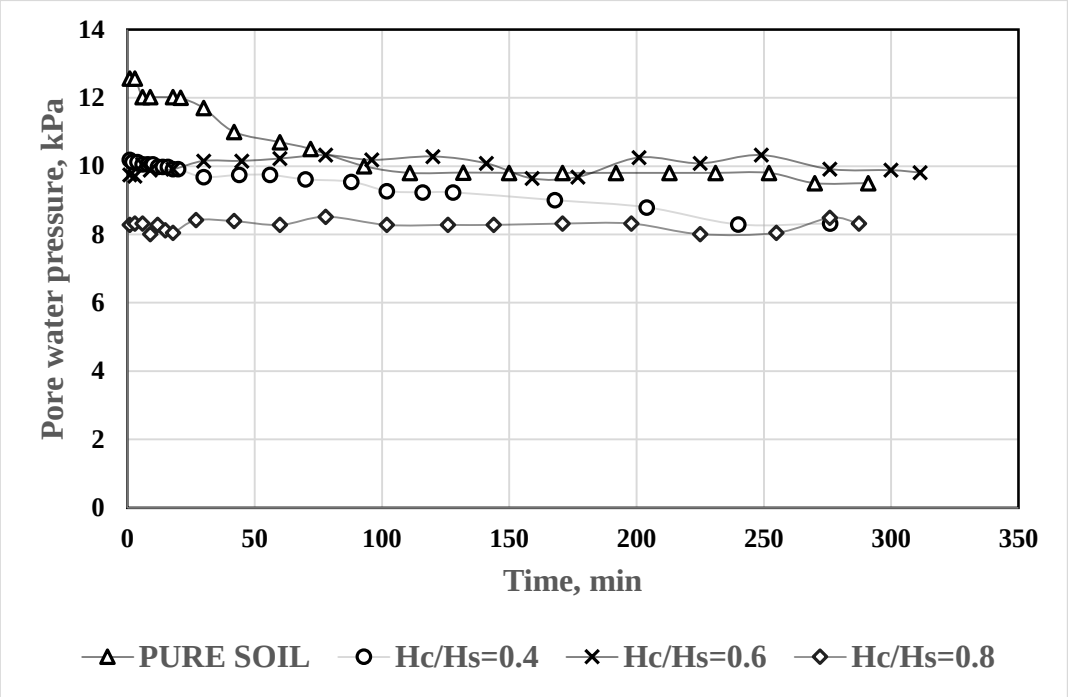

Fig. 5 Excess pore water pressure (As = 4%)

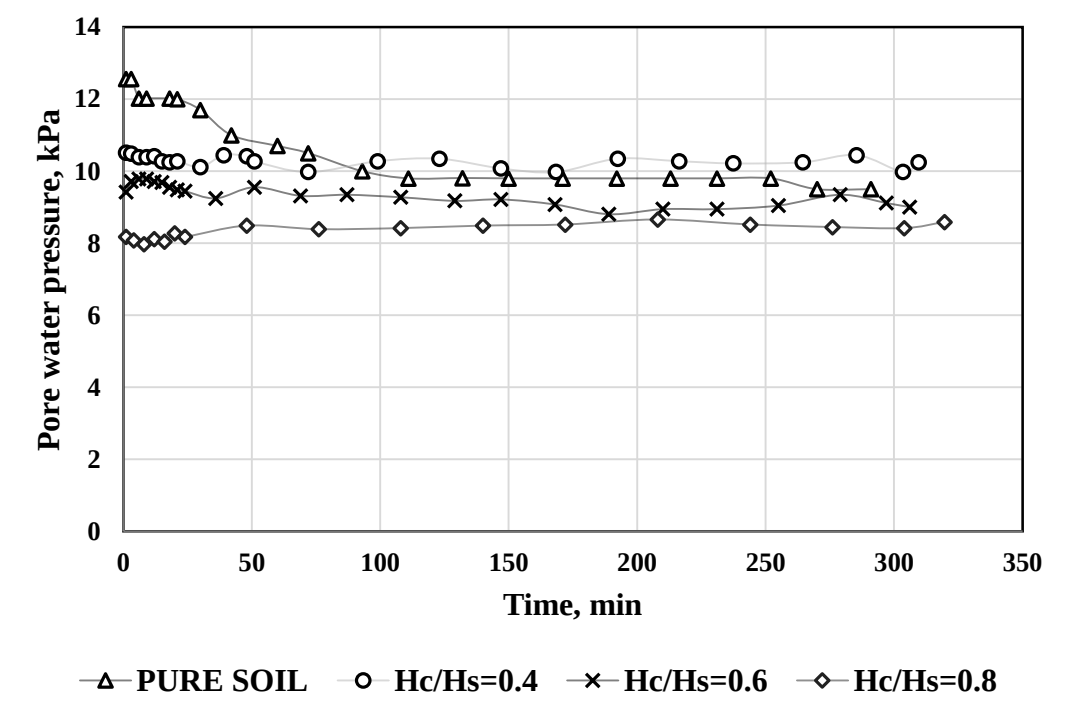

Fig. 6 Excess pore water pressure (As = 7.3%)

to 200 kPa from 120 kPa, representing a Ko of 0.61. After waiting for the dissipation of pore water pressure and water drainage to stop, the creep settlement was embiggened and recorded with time. This was conducted to benefit the features of this test by simulation of the one-dimensional consolidation test inside the triaxial cell and represent a unit cell concept under Ko condition in addition to allowing for a surcharge during independent footing load. The third and final stages of testing involved applying separate foundation loading under undrained conditions. Table 2 summarizes the testing program.

3. Results and discussion

The secondary consolidation settlement is associated

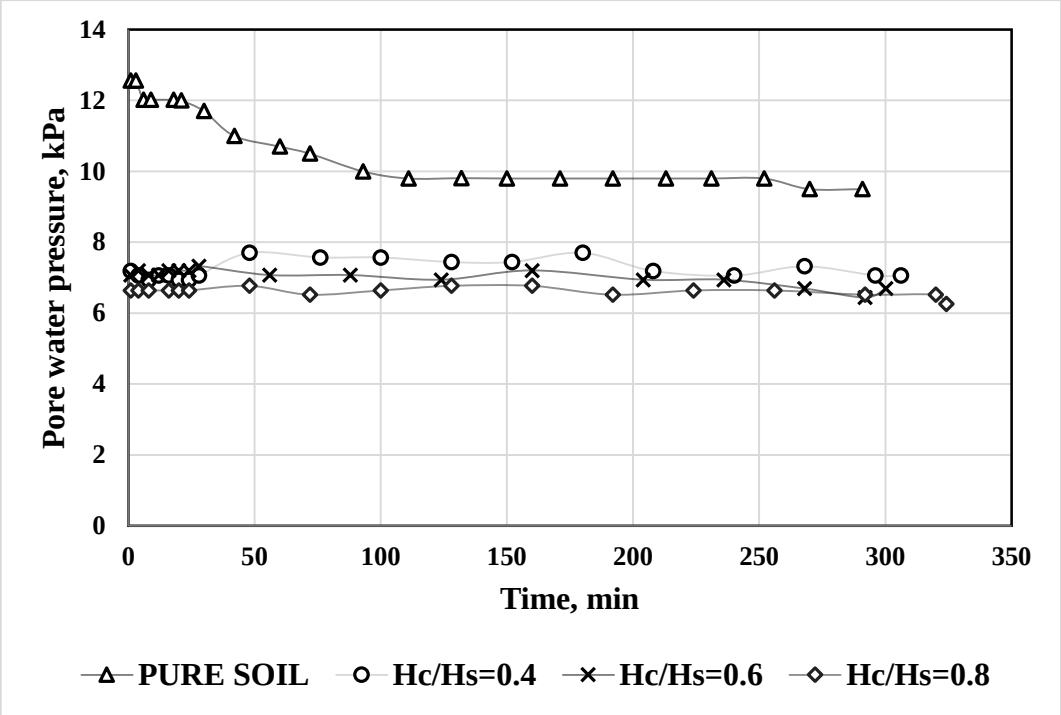

Fig. 7 Excess pore water pressure (As=14.4%)

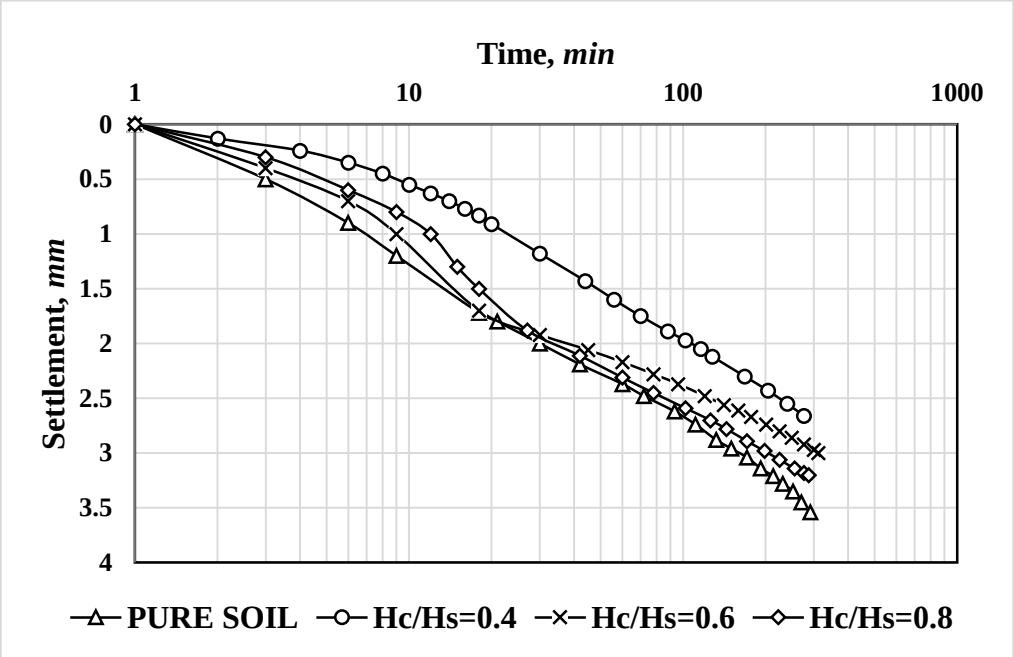

Fig. 8 Settlement – time relationship for model stone columns with As = 4%

with dissipation of excess pore water pressure and stopping of the volumetric strain of the sample under drained conditions; the pore water pressure during testing was recorded and shown in Figs. 5 to 7.

The change in stress of the column and surrounding soil under the top of the sample was observed during the apparent Ko consolidation. The findings of the reinforced 20, 27 and 38 mm diameter columns, 80 mm, 120 mm and 160 mm in length, are seen in the figures. Figures show that the vertical stress for the apparent Ko loading increased by 80 kPa.

Figs. 5 to 7 show that the pore water pressure developed in the model of the natural soil is greater than models using stone column which ascertains that the stone column accelerated the dissipation of excess pore water pressure.

Hameedi *et al*. (2021) noted that the value of pore water pressure is not equal to the applied vertical stress, because part of the applied stress goes to solid particles. Part of

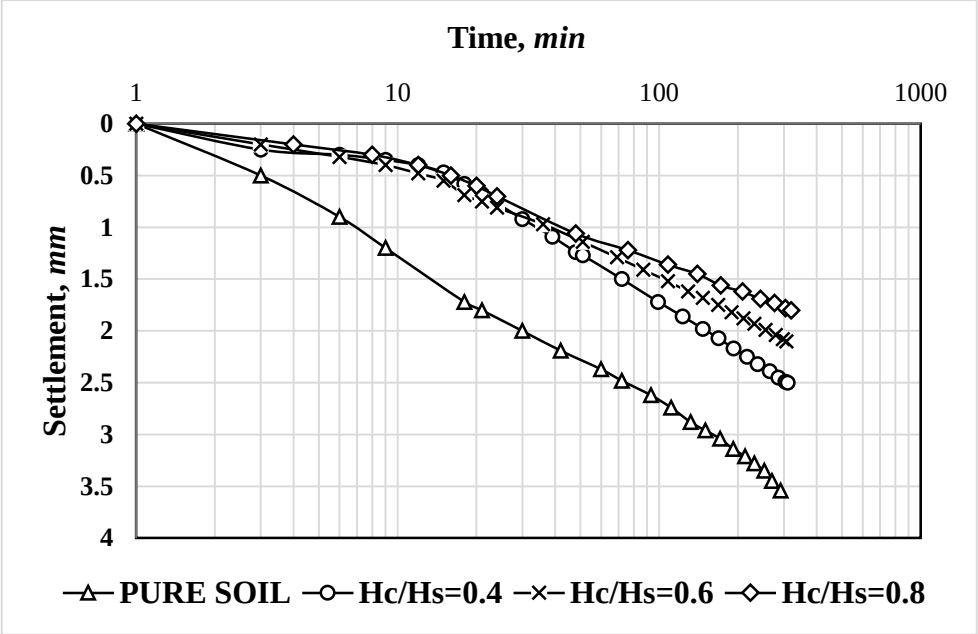

Fig. 9 Settlement – time relationship for model stone columns with As = 7.3%

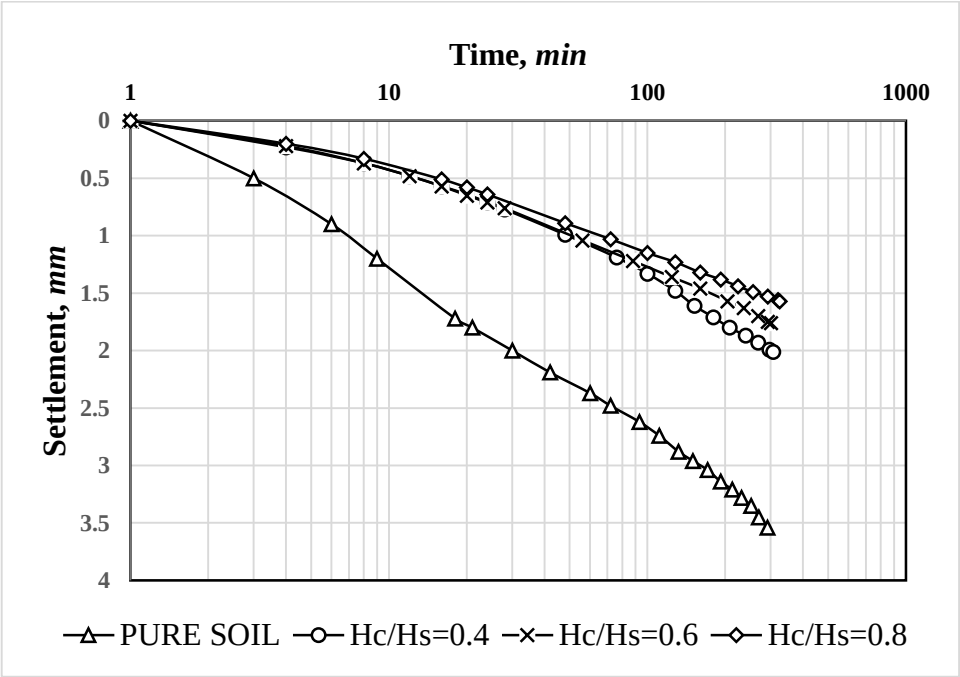

Fig. 10 Settlement – time relationship for model stone columns with As = 14.4%

stress causes sliding of solid particles on the sample, and this sliding explains the relaxation of stress when it happens.

Figs. 8 to 10 display the time-displacement characteristics of the constructed columns with partial penetration of 0.4, 0.6 and 0.8 diameters of columns 20, 27 and 38 mm, respectively having As = 4%, 7.3% and 14.4%.

Figs. 8 to 10 highlight the effect of area ratio in decreasing the model footing settlement. Fo example, the model with As 14.4% resulted in a decrease in settlement of (12.9 – 129.0)% compared to (11.1 – 33.3)% for model with As 4%.

Table 3 presents the corresponding creep improvement factor for each test. The creep improvement ratio (n_{creep}) is also specified for all As values in Fig. 11 with the l/d ratio. where

$$n_{creep}=\frac{\delta_{untreated}}{\delta_{treated}} \quad (1)$$

It is seen that there is a rapid increase in the creep improvement factor with (l/d) for model with As = 14.4%.

Fig. 12 is also drawn for the creep improvement factor increase with the area replacement ratio. It is evident that

Table 3 Creep improvement factor

Test No	Secondary settlement gradient, δ	Creep Improvement Factor, n_{creep}	Degree of Improvement, %
T-01	1.706	1	0
T-02	1.563	1.09	8.38
T-03	1.16	1.47	32
T-04	1.308	1.3	23.33
T-05	1.571	1.09	7.91
T-06	1.233	1.38	27.73
T-07	0.899	1.9	47.3
T-08	1.267	1.35	25.73
T-09	0.987	1.73	42.15
T-10	0.819	2.08	51.99

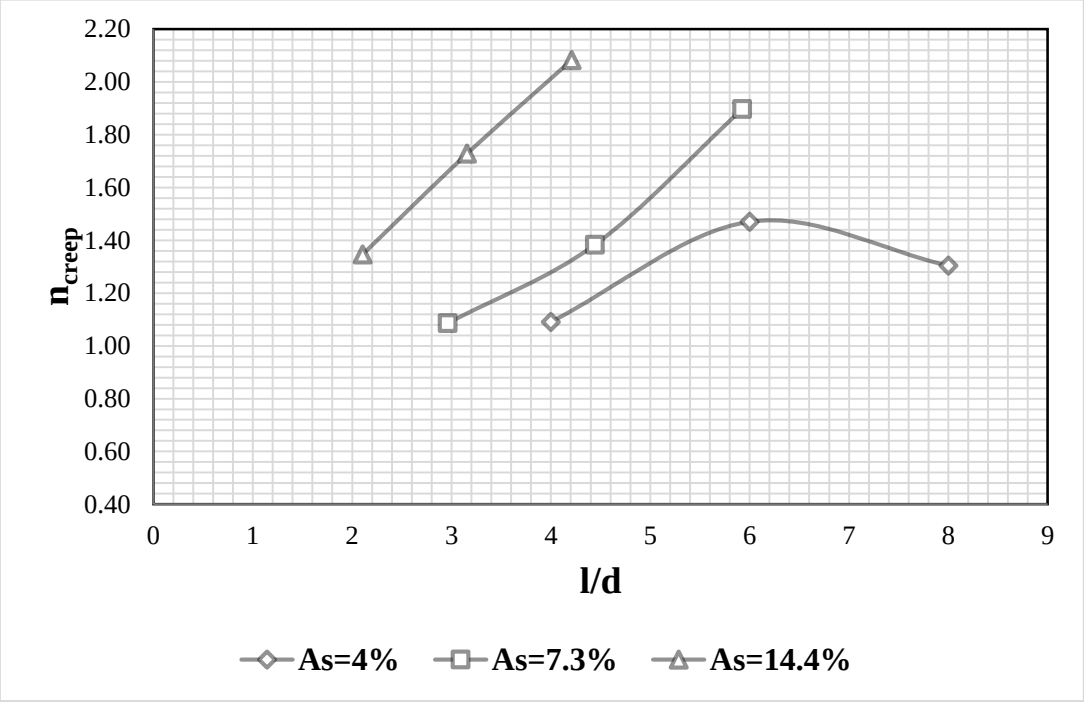

Fig. 11 Creep improvement factor variation with l/d

with the increase of the area replacement ratio, the settlement improvement factor increases.

The degree of improvement is varying from 12.4 to 55% according to the area replacement ratio and (l/d) ratio, as shown in Table 4.

The microstructural makeup of clays has a significant impact on the mechanisms involved in creep. Rigid aggregates undergo translation and rotation as a result of shearing, along with the disintegration of a specific number of particle linkages, which results in the creation of slip units, which are collections of parallel flaky particles.

In the creep scenario, the granular column experiences a vertical stress transfer from the moving soil. Total settlement improvement factors are lower than their primary equivalents because of increased yielding caused by the additional vertical tension transferred to the already yielded column.

Columns inhibited long-term creep settlement, although not as much as primary settlement, according to McCabe *et al.* (2009).

As illustrated in Table 4, an improvement in creep settlement can result in 50% when using stone columns with As = 14.4%.

Sexton *et al.* (2016) found that increased settlement leads to a reduction in the bonding parameter, χ. Creep (i.e. more settlement) leads to additional bonddegradation (for both the untreated and treated cases), andhence a larger reduction in χ. For the 'no creep' case, columns reduce settlement to a larger extent than they do for the 'creep' case (and hence they curtail the amount by which χ is reduced).

Lower "total" settlement improvement factors—that is, variables that are lower than main settlement improvement factors—are the result of incorporating creep. The primary and creep settlement improvement factors, which are significantly smaller than the former but still greater than unity, are combined to generate the total settlement improvement factors, which are essentially a weighted average of them. Lower settlement improvement factors for creep settlements should be employed in the design process if creep accounts for a sizable fraction of total settlement.

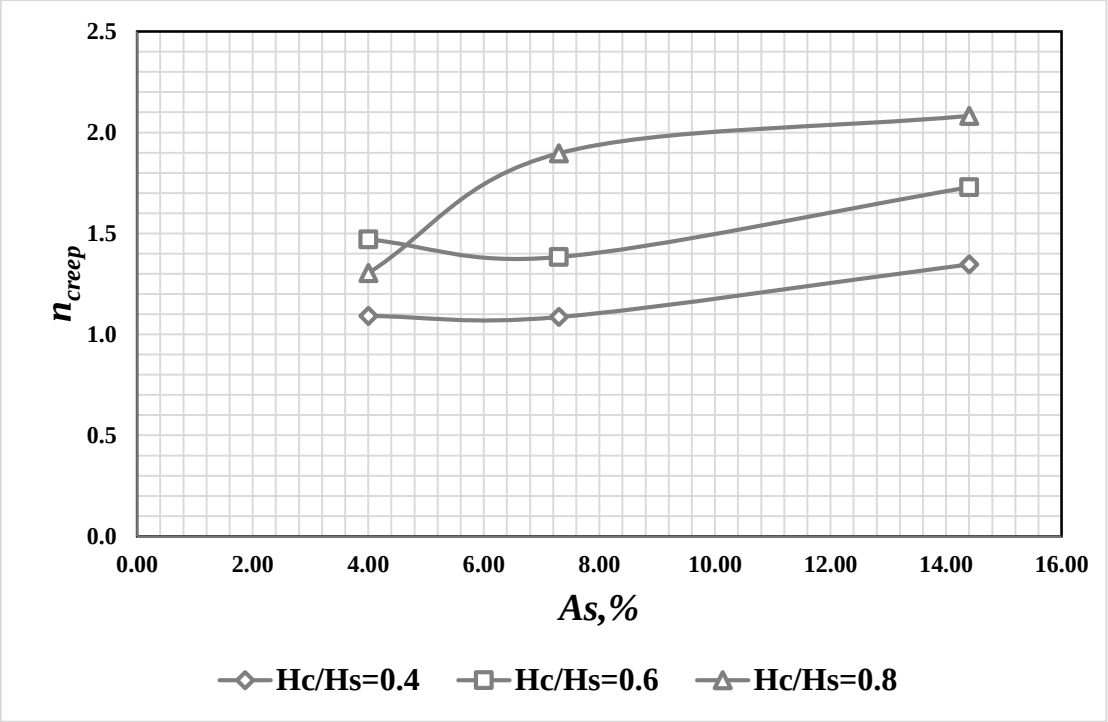

Fig. 12 Variation of the creep improvement factor variation with the area ratio

Table 2 Degree of improvement of tests

Test	Column length, l (mm)	Column diameter, d (mm)	l/d	Area replacement ratio, As (%)	Degree of improvement, %
T-01	0	0	0	0	0
T-02	**80**	**20**	4.00	**4**	8.38
T-03	**120**	**20**	6.00	**4**	32
T-04	**160**	**20**	8.00	**4**	23.33
T-05	**80**	**27**	2.96	**7.3**	7.91
T-06	**120**	**27**	4.40	**7.3**	27.73
T-07	**160**	**27**	5.90	**7.3**	47.3
T-08	**80**	38	2.10	**14.4**	25.73
T-09	**120**	38	3.16	**14.4**	42.15
T-10	**160**	38	4.20	**14.4**	51.99

4. Conclusions

This paper describes the results of improvement of organic soil by means of floating, isolated stone columns tested inside a triaxial cell. The significant findings of this work include:

1. Generally, the secondary settlement of footing on stone column in organic soil decreases as the A_s, *l/d and* H_c/H_s increase because of the stiffness increment of the composite ground. The model with As 14.4% resulted in a decrease in settlement of (12.9 – 129.0)% compared to (11.1 – 33.3)% for model with As 4%.
2. For area replacement ratio (A_s =4%), the degree of improvement is directly proportional to the (*l/d*) ratio; until it reaches (*l/d* =6), then it begins to decline, while there is a rapid increase in the creep improvement factor with (l/d) for model with As = 14.4%.
3. The degree of improvement in creep settlement using stone columns in organic clay is varying from 8 to 51% according to the area replacement ratio and (*l/d*) ratio.
4. The pore water pressure developed in the model of the natural soil is greater than models using stone column which proves that the stone column accelerated the dissipation of excess pore water pressure.

5. Limitations

The work described in this article deals with some limits associated with previous investigating and using reduced physical scale models to provide an insight into the settlement behavior of isolated stone columns in addition to limited height and diameter of the spacemen that can be used.

References

Aboshi, H. (1979), "The Compozer"-a method to improve characteristics of soft clays by inclusion of large diameter sand columns", *Proceedings of the international conference on soil reinforcement: Reinforced earth and other techniques*, Paris, **1**, 211-216.

Ambily, A.P. and Gandhi, S.R. (2007), "Behavior of stone columns based on experimental and FEM analysis", *J. Geotech. Geoenviron. Eng.*, 133(4), 405-415. https://doi.org/10.1061/(ASCE)1090-0241(2007)133:4(405).

Al-Auqbi, S.T., Salim, N.M. and Mahmood, M.R. (2022), "The impact of using different types of soft soils treated by stone columns on creep behavior", *Proceedings of the IOP Conf. Ser.: Earth Environ. Sci*., **961**, 012052. https://doi.org/10.1088/1755-1315/961/1/012052.

ASTM, D422 (2007), Standard test method for particle-size analysis of soils, American Society for Testing and Materials.

ASTM, D2435 (2004), Standard Test Methods for One-Dimensional Consolidation Properties of Soils Using Incremental Loading, American Society for Testing and Materials.

ASTM, D2974 (2020), Standard Test Methods for Determining the Water (Moisture) Content, Ash Content, and Organic Material of Peat and Other Organic Soils, American Society for Testing and Materials.

ASTM, D4318 (2018), Standard Test Methods for Liquid Limit, Plastic Limit, and Plasticity Index of Soils.

ASTM, D4767 (2011), Standard Test Method for Consolidated Undrained Triaxial Compression Test for Cohesive Soils, American Society for Testing and Materials.

Balaam, N.P. and Booker, J.R. (1981), "Analysis of rigid rafts supported by granular piles", *Int. J. Numer. Anal. Method. Geomech*., **5**(4), 379-403.

Barksdale, R.D. and Bachus, R.C. (1983), "Design and construction of stone columns", Appendixes. Federal Highway Administration.

Basha, A., Azzam, W. and Elsiragy, M. (2024), "Utilization of sand cushion for stabilization of peat layer considering dynamic response of compaction". *Civil Eng. J.*, 10(4), https://doi.org/10.28991/CEJ-2024-010-04-011.

Castro, J., Karstunen, M., Sivasithamparam, N. and Sagaseta, C. (2013), "Numerical analyses of stone column installation in Bothkennar clay", *Proceedings of the International Conference on Installation Effects in Geotechnical Engineering (ICIEGE)*, Rotterdam, the Netherlands.

Fattah, M.Y., Shlash, K.T. and Al-Waily, M.J.M. (2011), "Stress concentration ratio of model stone columns in soft clays", *Geotech. Test. J.*, **34**(1), 50-60. https://doi.org/10.1520/GTJ103060.

Fattah, M.Y., Zabar, B.S. and Hassan, H.A. (2015), "Soil arching analysis in embankments on soft clays reinforced by stone columns", *Struct. Eng. Mech.*, **56**(4), 507-534. https://doi.org/10.12989/sem.2015.56.4.507.

Fattah, M.Y., Zabar, BS. and Hassan, H.A. (2016),. "Experimental analysis of embankment on ordinary and encased stone columns", *Int. J. Geomech*., **16**(4), 04015102. https://doi.org/10.1061/(ASCE)GM.1943-5622.0000579.

Fattah, M.Y., Al-Neami, M.A. and Al-Suhaily, A.S. (2017), "Estimation of bearing capacity of floating group of stone columns", *Eng. Sci. Tech. Int. J.*, **20**(3), 1166-1172. https://doi.org/10.1016/j.jestch.2017.03.005.

Fattah, M.Y., Al-Omari, R.R. and Hameedi, M.K. (2021), "Tracing of stresses and pore water pressure changes during a multistage modified relaxation test model on organic soil", *Arabian J. Geosci.*, **14**, 1976. https://doi.org/10.1007/s12517-021-08321-7.

Feng, W.Q. and Yin, J.H., (2020), "Development and verification of a new simplified method for calculating settlement of a thick soil layer with nonlinear compressibility and creep", *Int. J. Geomech. ASCE*, 20(3). https://doi.org/10.1061/(ASCE)GM.1943-5622.0001562.

Feng, R., Wang, L., Wei, K. and Zhao, J., (2021), "Consolidation settlement of soil foundations containing organic matters subjected to embankment load", *Geomech. Eng*., **24**(1), 43-55. https://doi.org/10.12989/gae.2021.24.1.043.

Hameedi, M.K., Fattah, M.Y. and Al-Omari, R.R., (2020), "Creep characteristics and pore water pressure changes during loading of water storage tank on soft organic soil", *Int. J. Geotech. Eng*., **14**(5), 527–537, https://doi.org/10.1080/19386362.2019.1682350.

Hughes, J.M.O. and Withers, N.J. (1974), "Reinforcing of soft cohesive soils with stone columns", *Ground Eng*., **7**(3).

Kumar, G. and Samanta, M. (2020), "Experimental evaluation of stress concentration ratio of soft soil reinforced with stone column", *Innov. Infrastruct. Solut*., https://doi.org/10.1007/s41062-020-0264-6.

Lajevardi, S.H. and Enami, S. (2021), "Small scale behavior of stone columns encased by tires", *Geomech. Eng*., **25**(5), 429-438. https://doi.org/10.12989/gae.2021.25.5.429.

McCabe, B.A., Nimmons, G.J. and Egan, D. (2009), "A review of field performance of stone columns in soft soils", *Proceedings of the Institution of Civil Engineers-Geotechnical Engineering*, **162**(6), 323-334. https://doi.org/10.1680/geng.2009.162.6.323.

McKelvey, D. (2002), "The performance of vibro stone column reinforced foundations in deep soft ground", Ph.D. thesis, Queen's University Belfast.

McKelvey, D., Sivakumar, V., Bell, A. and Graham, J. (2004), "Modelling vibrated stone columns in soft clay", *Proceedings of the Institution of Civil Engineers-Geotechnical Engineering*, **157**(3), 137-149. https://doi.org/10.1680/geng.2004.157.3.137.

Mitchell, J.K. and Huber, T.R. (1985), "Performance of a stone column foundation", *J. Geotech. Eng*., **111**(2), 205-223.

Mitchell, J.K. and Kelly, R. (2013), "Addressing some current challenges in ground improvement", *Proceedings of the Institution of Civil Engineers, Ground Improvement*, **166**(3), 127e37. https://doi.org/10.1680/grim.12.00030.

Mohamed, M.K., Sakr, M.A. and Azzam, W.R. (2023), "Geotechnical behavior of encased stone columns in soft clay soil", **8**, 80. https://doi.org/10.1007/s41062-023-01044-6.

Priebe, H. (1976), "Estimating settlements in a gravel column consolidated soil", *Die Bautechnik*, **53**, 160-162.

Priebe, H.J. (1995), "The design of vibro replacement", *Gound Eng.* **28**(10), 31.

Shahu, J.T., Madhav, M.R. and Hayashi, S. (2000), "Analysis of soft ground-granular pile-granular mat system", *Comput. Geotech*., **27**(1), 45-62. https://doi.org/10.1016/S0266-352X(00)00004-5.

Sexton, B.G., McCabe, B.A., Karstunen, M. and Sivasithamparamc, N. (2016), "Stone column settlement performance in structured *anisotropic clays: the influence of creep", J. Rock Mech. Geotech. Eng.*, **8**(5), 672-688, https://doi.org/10.1016/j.jrmge.2016.05.004.

Sun, J., Lu, M., Xu, B. and Shan, J. (2024), "Consolidation of high replacement ratio stone column-reinforced ground: Analytical solutions incorporating clogging effect", *J. Rock Mech. Geotech. Eng*., https://doi.org/10.1016/j.jrmge.2023.12.011.

Van Impe, W. (1983), "Improvement of settlement behaviour of soft layers by means of stone columns", *Proceedings of the 8th European Conference on Soil Mechanics and Foundation Engineering: Improvement of Ground*.

Watts, K.S., Johnson, D., Wood, L.A. and Saadi, A. (2000), "An instrumented trial of vibro ground treatment supporting strip foundations in a variable fill", *Géotechnique*, **50**(6), 699-708.

https://doi.org/10.1680/geot.2000.50.6.699.
Ye, W.M., Lai, X.L., Wang, Q., Chen, Y.G., Chen, B. and Cui, Y.J. (2014), "An experimental investigation on the secondary compression of unsaturated GMZ01 bentonite", *Appl. Clay Sci.*, **97-98**, 104-109. https://doi.org/10.1016/j.clay.2014.05.012.

CC

Notation

A_c	Area of stone column
A_s	Area replacement ratio
B	Skempton's pore water pressure parameter
c_c	Compression index
c_s	Swelling index
c_u	Undrained shear strength
c_α	Secondary compression index
D	Foundation diameter
d	Stone column diameter
E_c / Es	Deformation ratio of soil and column
H_c/H_s	Column length to sample height ratio
K_o	Earth pressure coefficient at rest
L	Length of stone column
LL	Liquid limit
l/d	The ratio of column length to diameter
LOI	Loss of Ignition (organic matter)
n_{creep}	Creep improvement factor
PI	Plasticity index
PL	Plastic limit
s	Column spacing
$\delta_{treated}$	Creep gradient of treated soil
$\delta_{untreated}$	Creep gradient of untreated soil
σ_3	Confining pressure
v_c	Poisson's ratio of granular column
v_s	Poisson's ratio of soil
ϕ	Friction angle of soil